CME Geometry Deduced from Cosmic Ray Anisotropy

K. Munakata,[1] T. Kuwabara,[1] J. W. Bieber,[2] S. Yasue,[1] C. Kato,[1] S. Akahane,[1] M. Koyama,[1] P. Evenson,[2] R. Pyle,[2] Z. Fujii,[3] M. L. Duldig,[4] J. E. Humble,[5] M. R. Silva,[6] N. B. Trivedi,[6] W. D. Gonzalez,[6] and N. J. Schuch[6]
(1) Physics Department, Shinshu University, Matsumoto 390-8621, JAPAN
(2) Bartol Research Institute, University of Delaware, Newark, DE 19716, USA
(3) STE Laboratory, Nagoya University, Nagoya 464-8601, JAPAN
(4) Australian Antarctic Division, Kingston, Tasmania 7050, AUSTRALIA
(5) School of Mathematics and Physics, University of Tasmania, Hobart, Tasmania 7001, AUSTRALIA
(6) Southern Regional Space Research Center, National Institute for Space Research (OES/CRSPE/INPE), Santa Maria, RS, BRAZIL

Abstract

The geometry of the cosmic-ray depleted region formed behind the shock associated with the CME is derived for each of two events that occurred in April 11 and August 27, 2001 by analyzing the cosmic-ray anisotropy observed by a global network of muon detectors. The preliminary analysis based on a simple model for the density distribution in space tells us that the temporal variation of the observed spatial gradient of cosmic-ray density is consistent with the depleted region confined in an inclined "cylinder" approaching and then leaving the earth with a constant velocity. The orientation of the axis, the thickness and the propagation speed of the cylinder are obtained for each event. This is the first result deriving the three dimensional geometry of the cosmic-ray depleted region from the observation of high energy cosmic rays by muon detectors.

1. Data analysis

We analyze the pressure-corrected hourly count rates of cosmic-rays recorded by three multidirectional muon detectors at Nagoya (Japan), Hobart (Australia) and São Martinho (Brazil), which compose a prototype network covering a wide range of viewing directions over the earth [1, 2]. In the prototype network, the total 35 directional channels have been continuously monitoring the intensity of cosmic rays with median rigidities ranging from 53 to 119 GV. By analyzing the data, we first derive the cosmic ray density (or isotropic component of intensity) as a function of time t and three components of the anisotropy vector in space, $\boldsymbol{\xi}^{(W)}(t)$, corrected for the solar-wind convection streaming. From the obtained $\boldsymbol{\xi}^{(W)}(t)$, we then calculate the fractional gradient $\mathbf{G}_{\perp}(t)$ (%/AU)

pp. 3561–3564

perpendicular to the IMF, as

$$\mathbf{G}_{\perp}(t) = -\mathbf{b}(t) \times \boldsymbol{\xi}^{(W)}(t)/R_L(t) \quad (1)$$

where $R_L(t)$ is the particle Larmor radius in AU and $\mathbf{b}(t)$ is a unit vector in the direction of the IMF. We used 1-hour averages of the *ACE* plasma data (Level 2), lagged by 1 hour as a rough correction for the solar wind transit time between the *ACE* satellite and the earth [3]. The unit vector $\mathbf{b}(t)$ also used *ACE* data lagged by 1 hour. For this part of our analysis, readers can refer to [2].

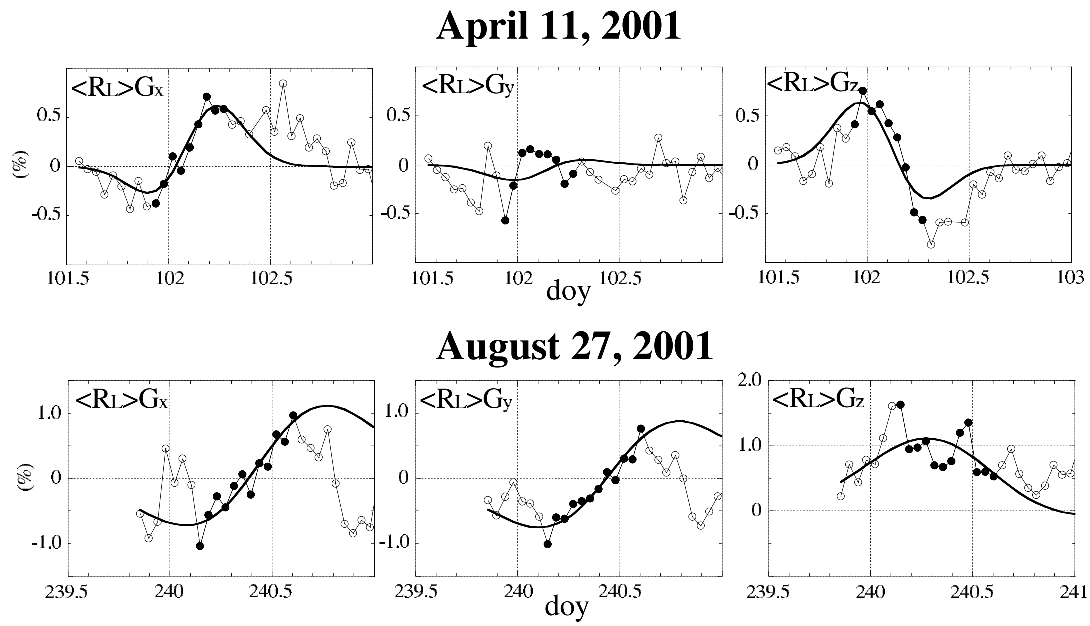

Fig. 1. Three components of the observed density gradient vector in the GSE coordinate system as functions of the day of year (doy). The observed gradients multiplied by the average Larmor radius ($\langle R_L \rangle$) of 50 GV primary particle are shown for the April event (top) and the August event (bottom). The data during the analyzed periods are plotted by full circles. The gradients reproduced by the cylinder model with the best-fit parameters in Table 1 are shown by solid curves (see text).

Fig.1 shows the temporal variations of $G_x(t)$, $G_y(t)$ and $G_z(t)$, three components of $\mathbf{G}_{\perp}(t)$ in the geocentric solar ecliptic (GSE) coordinate system, observed in association with two CME events that occurred in April 11 (top) and August 27 (bottom), 2001. It is clearly seen in this figure that the $G_x(t)$ component (in the left panel) systematically turns from negative to positive in both of these two events, indicating the cosmic-ray depleted region approaching and then leaving the earth. The $G_z(t)$ component (in the right panel), on the other hand, turns from positive to negative in April event, while it remains positive in August event. In this paper, we analyze the periods when the observed gradient plotted by full circles show systematic variations, on the basis of the following simple model.

We assume an axisymmetric spatial distribution for the cosmic-ray density with the minimum located along the axis of a straight "cylinder", which is an idealized model of a local section of a loop structure. Due to this axisymmetric distribution, the negative density gradient ($-\mathbf{G}_\perp$) observed at the earth directs perpendicular to the cylinder axis and toward the Closest Axial Point (CAP) on the axis. For our first step, we assume a simple gaussian function for the distribution, as

$$I(\rho) = I_0 e^{-\rho^2/2\lambda^2} \tag{2}$$

where ρ is the distance between the CAP and the earth, I_0 is the maximum density suppression in % and λ is a scale parameter representing the "thickness" of the cylinder. The magnitude $G(\rho)$ of the gradient is then given as

$$G(\rho) = -\frac{\rho}{\lambda^2} I_0 e^{-\rho^2/2\lambda^2} \tag{3}$$

By using the observed magnitude of the gradient for $G(\rho)$, we can deduce the distance ρ of the CAP from the earth by Equation (3) and get the GSE coordinates of the CAP every hour. We then obtain the apparent velocity vector, $\mathbf{V}_{app}$, of the CAP by fitting a linear function of t to each of the coordinates of the CAP. As the cylinder moves with the constant velocity ($\mathbf{V}_{cyl}$), the CAP observed from the earth also moves with the apparent velocity $\mathbf{V}_{app}$. We assume that $\mathbf{V}_{cyl}$ is parallel to the average solar wind velocity over the analyzed period. The velocity of the CAP ($\mathbf{V}_{axis}$) along the cylinder axis can be derived, as

$$\mathbf{V}_{axis} = \mathbf{V}_{app} - \mathbf{V}_{cyl} \tag{4}$$

The magnitude of $\mathbf{V}_{cyl}$ is determined to keep the obtained $\mathbf{V}_{axis}$ perpendicular to $\mathbf{V}_{app}$. We performed these calculations using various combinations of the parameters I_0 and λ, and find a pair of parameters minimizing the difference between the observed and reproduced gradients. The best-fitted gradients are shown by solid curves in Fig.1. As seen in the figure, a reasonable fitting results even from such a simple model.

2. Results and Conclusions

On the basis of a simple cylinder model for the cosmic-ray depleted region formed behind an interplanetary shock, we performed best-fit modeling of the cosmic-ray density gradients derived from the observations of the cosmic-ray anisotropy by a prototype network of muon detectors. The best-fit parameters derived from the preliminary analysis are summarized in Table 1 for each of two

CME events in Fig.1. In both events, G_x turned its sign from negative to positive indicating the cylinder approaching and then leaving the earth. In the April event, G_z also changed its sign. This indicates that the cylinder is inclined in the x-z plane by about 40° from the ecliptic plane. In the August event, on the other hand, G_y changed its sign indicating that the cylinder projection on the x-y plane is inclined. The CAP passed south of the earth in this event, as G_z remained positive throughout the analyzed period. The derived speed V_{cyl} (1430 km/s) of the cylinder in the April event is much faster than the solar wind speed (696 km/s) averaged over the analyzed period and also faster than V_{cyl} in the August event. This is manifested by the faster temporal variation of the gradient in the April event than that in the August event, as seen in Fig.1. Such high speed propagation is consistent with the time between the flare on the Sun and the SSC at the earth for this event.

Best-Fit parameters	April 11, 2001	August 27, 2001
I_0	-1.93 %	-0.95 %
λ	0.088 AU	0.060 AU
V_{cyl}	1430 km/s	425 km/s
GSE latitude and longitude of the cylinder axis	40.7°, 354.5°	30.0°, 319.0°

Table 1. The best-fit parameters obtained from analyses of the April and August events in Fig.1 (see text). The GSE latitude and longitude of the cylinder axis are derived from the orientation of $\mathbf{V}_{axis}$ defined in Equation (4).

3. Acknowledgements

This work is supported in part by U.S. NSF grants ATM-0000315 and ATM-0207196 and in part by the joint research program of the Solar-Terrestrial Environment Laboratory, Nagoya University. The muon observations at Nagoya and Hobart have been carried out by Shinshu University and Nagoya University in Japan, the University of Tasmania and the Australian Antarctic Division in Australia, while the prototype muon detector at São Martinho has been operated under collaboration between Shinshu University and the Southern Regional Space Research Center of National Institute for Space Research in Brazil. We thank N. F. Ness for providing *ACE* magnetic field and solar wind data via the *ACE* Science Center.

4. References

1. Munakata, K. et al. 2001, Proc. 27th ICRC, 9, 3494.
2. Munakata, K. et al. 2002, Adv. Space Res., submitted.
3. Bieber, J. W., and P. Evenson 1998, Geophys. Res. Lett., 25, 2955.